Journal of Power Sources 183 (2008) 604–608

Contents lists available at ScienceDirect

Journal of Power Sources

journal homepage: www.elsevier.com/locate/jpowsour

Short communication

Influence of preparation process on non-noble metal-based composite electrocatalysts for oxygen reduction reaction

Xuanying Deng[a,b], Xin Wang[a,*], Zi-Feng Ma[b]

[a] School of Chemical and Biomedical Engineering, Nanyang Technological University, Singapore 637459, Singapore
[b] Department of Chemical Engineering, Shanghai Jiaotong University, PR China

ARTICLE INFO

Article history:
Received 21 December 2007
Accepted 26 March 2008
Available online 22 May 2008

Keywords:
Non-noble electrocatalyst
Oxygen reduction reaction
Proton-exchange membrane fuel cell
Tetramethoxy-phenylporphyrin

ABSTRACT

Composite electrocatalysts based on the transition metal cobalt are synthesized for the oxygen reduction reaction (ORR) by mechanically mixing three basic precursors containing carbon black, cobalt acetate and tetramethoxy-phenylporphyrin (TMPP). The influence of various mixing processes, solvents, pyrolysis temperature and precursor ratios on the ORR activity of the electrocatalysts is investigated by means of their electrochemical characteristics. Levich–Koutecky plots show that the number of transferred electrons during ORR on these catalysts varies between 2 and 4. A pyrolyzed mixture synthesized by ultrasonication exhibits better activity for ORR than that prepared by ball milling. The solvent is found to have a significant effect on the performance of the catalysts in acidic media. The catalyst synthesized in water, a poor solvent of TMPP, has better activity than that synthesized in a good solvent of TMPP, such as *N*,*N*-dimethylformamide and acetic acid. The optimum pyrolysis temperature is 600 °C. Various mole ratios and Co/carbon weight ratios are examined. Maximum activity is found at a 1:1 TMPP/Co mole ratio and a 5% Co/carbon weight ratio.

1. Introduction

Because of their highly efficient energy conversion and low pollutant emissions, proton-exchange membrane fuel cells (PEMFCS) are now attracting enormous interest for various applications such as low/zero-emission vehicles, distributed home power generation, and power sources for small portable electronics [1,2]. One of the obstacles to the commercialization of PEMFCs is the high cost of the noble metals used as electrocatalysts, e.g., Pt [3]. Consequently, non-noble catalysts have been extensively investigated to replace Pt-based catalysts and to reduce the material cost of fuel cells [4,5].

During the past decades, most of the efforts to explore non-noble catalysts for oxygen reduction reaction (ORR) have focused on transition metal chalcogenides [6,7], oxides [8] and macrocycles [9–11]. In particular, the macrocyclic derivatives of cobalt and iron have been well characterized as promising alternative materials [12–15]. Nevertheless, these catalysts still suffer from low stability in an acidic environment and pyrolysis is found to improve the activity and stability significantly. The best electrocatalytic activity for ORR obtained with these precursors was observed with pyrolysis in the temperature range 500–700 °C. Another interesting catalytic site, labeled the high-temperature catalytic site, was also discovered at a higher pyrolysis temperature (≥800 °C). In the low temperature range, N_4-M/C was recognized as the active catalytic site, where C represents the carbon support. But at the high pyrolysis temperature (≥800 °C), the complete structure of the catalytic site is still unclear [16–18]. Dodelet and co-workers [19] proposed that $FeN_2C_4^+$ might be the catalytic site formed in the high-temperature range. Since the structure of the central MeN_4 chelate would be largely destroyed at such high pyrolysis temperatures, the metal complex might be only a precursor of the actual active material. The same author also found that both sites (N_4-M/C and N_2-M/C) were detected simultaneously at all pyrolysis temperatures [15]. Nonetheless, there is a consensus that the coexistence of carbon, nitrogen and Co (or Fe) sources is necessary for this composite catalyst to function. It is appealing to try to reproduce these electrocatalysts starting with different precursors of lower cost and easier availability, and to disclose the reasons for their activity so as to improve further their performance. Various transition metal precursors, nitrogen sources and carbon containing species have been investigated for this alternative preparation route and these three factors have proved to be critical for the formation of active catalyst sites such as N_4-metal or $FeN_2C_4^+$ [20,21]. For example, mechanical mixtures of the three key precursors were reported by Mocchi and Trasatti [21] to show remarkable catalytic activity in 1 M KOH aqueous solution and it was found that separating the nitrogen source

* Corresponding author. Tel.: +65 6316 8866; fax: +65 6794 7553.
E-mail address: WangXin@ntu.edu.sg (X. Wang).

0378-7753/$ – see front matter © 2008 Elsevier B.V. All rights reserved.
doi:10.1016/j.jpowsour.2008.03.092

from the metal one resulted in a better catalytic performance than pyrolyzed CoTMPP + carbon.

In our previous work [22], we found that pyrolyzed catalysts prepared by heating and refluxing of a dispersion consisting of tetramethoxy-phenylporphyrin (TMPP, porphyrin monomer), cobalt acetate and a carbon support in a microwave bath has good catalytic activity and stability. In this study, a systematic investigation is made of the effect of various synthesis parameters on the catalytic activity of the prepared catalyst, including mechanically mixing methods, solvents, and the ratio between the various components. To the knowledge of the authors, this is the first time that the influence of mechanically mixing methods and solvent effects have been investigated.

2. Experimental

The TMPP precursor was synthesized using the protocol as described elsewhere [23]. Carbon black Vulcan XC-72 (Cabot Corp.) was used as a carbon support. Cobalt nitrate hexahydrate (Merck Pte. Ltd.) was first mixed with TMPP in 12 mL solvent by stirring, followed by the slow addition of an appropriate amount of Vulcan XC-72. Then the dispersion was mechanical mixed either by ultrasonication or by ball milling for 1 h, followed by stirring for another 1 h at 80–90 °C. The powder resulting from evaporation of the solvent was finally crushed in an agate mortar and pyrolyzed in an argon atmosphere for 2 h. Three different solvents, i.e., water, acetic acid and *N*,*N*-dimethylformamide (DMF) were used to investigate the influence solvent of on the synthesized catalysts.

The catalytic activities of the prepared catalysts for ORR were characterized by means of a VMP2 Multichannel Potentiostat (Princeton Applied Research) in oxygen-saturated 0.5 M H_2SO_4. Platinum wire (diameter 1 mm) and a saturated calomel electrode (SCE) were used as a counter electrode and a reference electrode, respectively. All potentials are quoted versus the SCE. The working electrode was prepared as follows: about 8 mg of each catalyst sample were ultrasonically mixed in 1.5 mL of ultra pure water +0.1 mL of 5 wt.% Nafion to form a homogeneous ink. Then 5 μL of the ink was dropped on to the surface of a polished glass carbon electrode (diameter 3 mm) and dried in air. Linear scan voltammograms were recorded at scan rate of 5 mV s^{-1} between 0.8 and 0 V. The stability tests were carried out in an oxygen-saturated acidic medium at 25 °C by potentiostatic polarization at 0.4 V.

3. Results and discussion

Potentiodynamic curves of the catalysts synthesized by two different mixing methods namely ultrasonication (denoted as Cat-U) and ball milling (denoted as Cat-B) are presented in Fig. 1(a). The onset potential for ORR on Cat-B is close to that on Cat-U, but the latter has a higher limiting current which suggests different surface configurations formed during these two mixing processes. Disc polarization data at several rotation rates for the catalysts were used to construct Levich–Koutecky plots, as shown in Fig. 1(b). The results for a 50% Pt/C catalyst in the same medium is also presented for comparison. It is seen that the plots are straight lines with different slopes, confirming that the number of electrons (n) involved in the ORR depends on the electrocatalyst material. Values of n for the catalysts were calculated from the slope of the lines using:

$$I = 0.620\, nFA\, D_0^{2/3} w^{1/2} v^{-1/6} C_0 \quad (1)$$

where I is the limiting diffusion current density, F is the Faraday constant, D_0 is the oxygen diffusion coefficient, w is the rotation rate in rpm, v is the kinematic viscosity of the solution, and C_0 is the oxygen solubility in the electrolyte. A slight increase in the

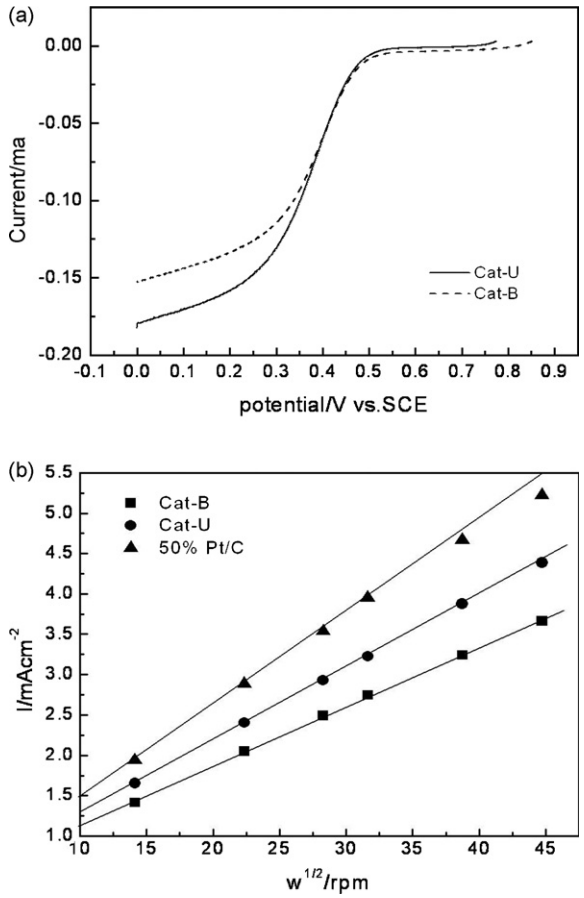

Fig. 1. (a) Potentiodynamic curves of ORR on Cat-US and Cat-B, measured at 5 m V s^{-1}, rotating rate 500 rpm in O_2-saturated 0.5 M H_2SO_4; (b) Levich–Koutecky plots for ORR on Cat-U and Cat-B catalysts compared with that obtained on 50% Pt/C in O_2-saturated 0.5 M H_2SO_4.

Levich–Koutecky slope for Cat-U compared with Cat-B can be noted. The calculated numbers of electrons are 2.7, 3.3 and 4.0 for Cat-B, Cat-U and 50% Pt/C, respectively. The ORR on Pt/C basically follows a four-electron mechanism, while a significant portion of the ORR on the two composite catalysts occur via a two-electron mechanism and Cat-U has better kinetics for ORR than Cat-B, as evidenced by the higher electron number. One reasonable explanation for this is a higher utilizable metal loading in the micropores of the carbon support during the ultrasonic process than during ball milling. It is proposed that catalytic sites for this type of catalyst are hosted in micropores [24]. Compared with ball milling, ultrasonication is more efficient in the removal of the trapped gas inside the micropores and is capable of fully wetting these micropores. Once wetted, these micropores then can be used for the impregnation of metal and nitrogen precursors, leading to greater number of active sites than are formed by ball milling.

Current-potential polarization curves are shown in Fig. 2 for pyrolyzed catalysts synthesized in water (denoted as Cat-W), acetic acid (denoted as Cat-A) and *N*,*N*-dimethylformamide (denoted as Cat-D). The half-wave potential, which is defined as the potential at which the measured current reaches half of the limiting current, decreases in the following order: Cat-W, Cat-D and Cat-A. The interesting feature is that TMPP is water insoluble but soluble in acetic acid and *N*,*N*-dimethylformamide. The superior activity of Cat-W indicates that the Me–N band in the active catalytic sites mainly forms on pyrolysis, and not during the mixing or dissolving step. To obtain a better understanding of the potential effect of these

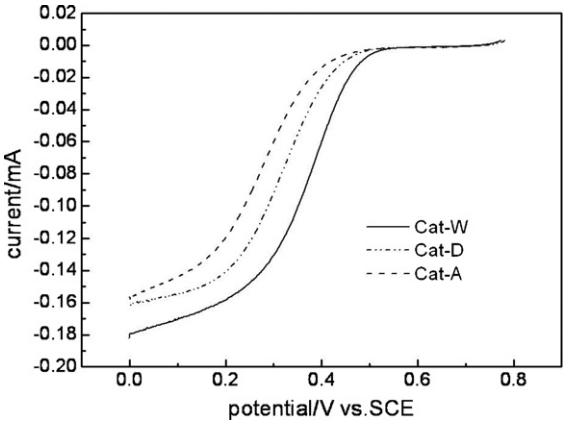

Fig. 2. Current-potential polarization curves for ORR on Cat-W, Cat-D and Cat-A, measured at 5 m V s^{-1}, rotating rate 500 rpm in O_2-saturated 0.5 M H_2SO_4.

solvents on the catalyst, the surface area was measured by nitrogen adsorption. As shown in Table 1, the composite catalysts all have a lower BET surface area than the support material Vulcan XC-72, because of the loading of TMPP and Co. It is found that the surface area of the catalyst synthesized in water is higher than that of the Cat-A and Cat-D catalysts. There is a very slight difference in surface area between Cat-A and Cat-D. By contrast, there is a large difference micropore surface area: Cat-W (114 m^2 g^{-1}) > Cat-D (101 m^2 g^{-1}) > Cat-A (70 m^2 g^{-1}), which shows the same trend as the catalytic activity. According to the literature data [25], the activity for ORR is found to be proportional to the post-pyrolysis microporous specific area. The catalytic sites for ORR may only form in the micropores of the carbon black and the density of the micropores in carbon black presently limits the density of active sites and the overall activity of catalysts. This statement agrees well with the observation that a catalyst with higher microporous area gives better activity. Different solvents have a different effect on the microporous specific area and, subsequently, the activity of catalysts through microporous surface area.

Heat treatment is another key step in the formation of active catalytic sites, since the Me—N_4 bond of the catalysts only forms during the pyrolysis process. The Cat-W catalysts pyrolyzed at various temperatures were tested for their activity for ORR. Typical ORR polarization curves in 0.5 M H_2SO_4 obtained on these catalysts are given in Fig. 3(a). Catalysts pyrolyzed at 600 and 800 °C exhibit the best activity and the activity slightly decreases when the temperature continues to increase. Thermogravimetric analysis (TGA) also demonstrats that the formation of N_4-metal active catalytic site for this composite catalyst starts at a lower temperature than 800 °C. Fig. 4 shows that Cat-W starts to pyrolyze at a lower temperature than CoTMPP. In the high-temperature range, where the high-temperature active catalytic site may form, Cat-W has a large weight loss from 685 °C, i.e., lower than 740 °C for CoTMPP. At the same time, a lower slope for Cat-W is seen in the temperature range 440–800 °C. This indicates that the active catalytic site of the composite materials is easier to form on this Cat-W catalyst than

Table 1
Surface area and micropore area of various materials measured by nitrogen adsorption

Catalysts	Area (m^2 g^{-1})	Micropore (m^2 g^{-1})
Vulcan XC-72	256	118
Cat-W	181	114
Cat-D	161	101
Cat-A	158	70

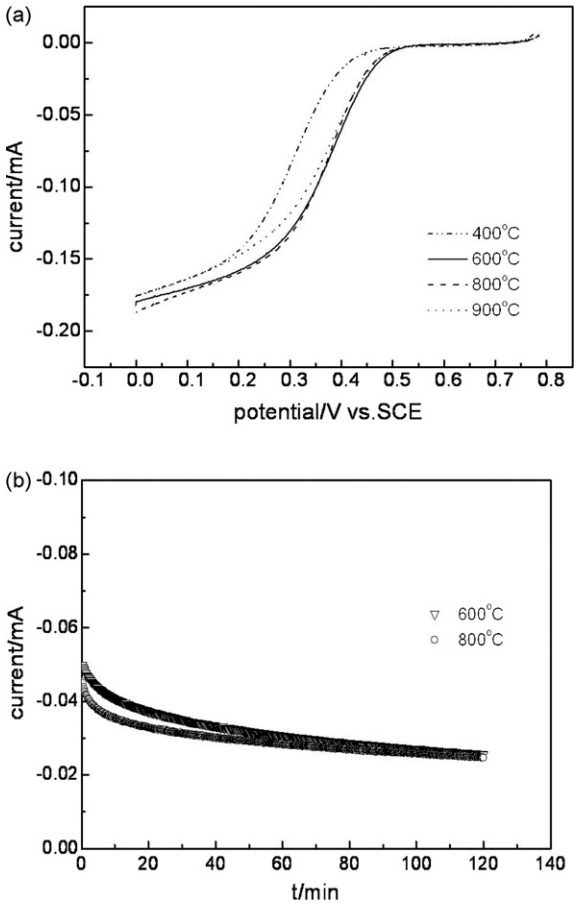

Fig. 3. (a) Potentiodynamic curve for ORR on catalysts pyrolyzed at 400, 600, 800 and 900 °C, measured at 5 m V s^{-1}, rotating rate 500 rpm in O_2-saturated 0.5 M H_2SO_4; (b) chronoamperometric curves for ORR on catalysts pyrolyzed at 600 and 800 °C, measured in O_2-saturated 0.5 M H_2SO_4 at 400 m V and rotating rate 500 rpm.

by the pyrolysis of CoTMPP. The chronoamperometric curve shown in Fig. 3(b) are for catalysts pyrolyzed at 600 and 800 °C, measured at 400 mV in oxygen saturated 0.5 M H_2SO_4, at a rotating rate of 500 rpm. Both catalysts show a similar current after 120 min. The initial current obtained for the catalyst synthesized at 600 °C is even slightly higher than that for 800 °C. Therefore, 600 °C is considered as the optimum pyrolysis temperature.

The content of the metal is very important for the activity of catalysts and the low utilizable metal loading is considered as the

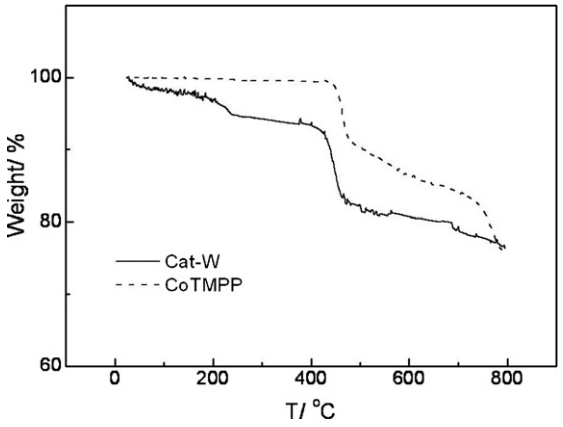

Fig. 4. TGA curves of Cat-W and CoTMPP.

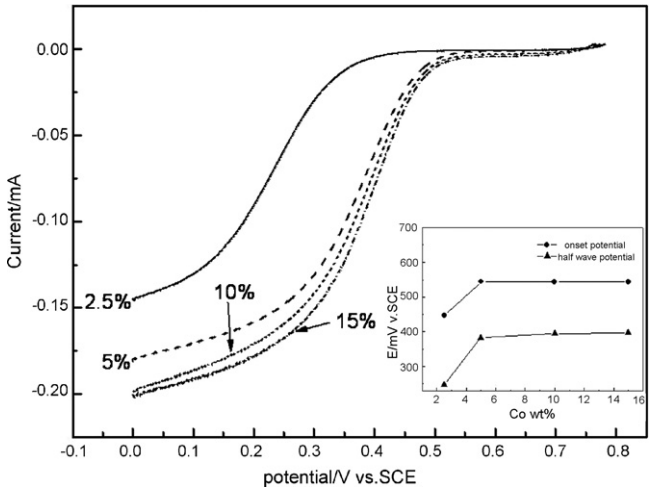

Fig. 5. Potentiodynamic curves for ORR on catalysts with different contents of Co. Inset shows change of onset potential and half-wave potential vs. content of Co.

major impediment to the replacement of platinum in PEMFCs [26]. Here, we have studied the effect of metal loading on this composite catalyst in an attempt to identify an optimum content of the metal. Potentiodynamic curves for ORR on catalysts with different loadings of Co are given in Fig. 5. These catalysts were synthesized in water through ultrasonication and pyrolyzed at 600 °C. It is found that the onset potential and the half-wave potential value increase when the metal loading increases from 2.5 to 5 wt.% (Co/C). Further increase in the Co content has a negligible effect. In such a synthesis condition, the utilizable metal loading increases slowly and levels off when the nominal value reaches 5 wt.% (Co/C). Taking the material cost into consideration, the optimum metal content of this catalyst is 5 wt.% (Co/C).

Nitrogen sources are also critical to catalytic activity. It is clear that the most important factor is the utilizable nitrogen content of the materials. A higher content of pyridinic-type nitrogen bonded with metal yields a higher density of catalytic sites and a better electrocatalyst. Current-potential polarization curves of catalysts with different nitrogen contents are presented in Fig. 6. The best activity is obtained at TMPP:Co = 1:1 with both the onset potential and the half-wave potential reaching the highest values. This is in good agreement with the literature data [20] in alkaline media,

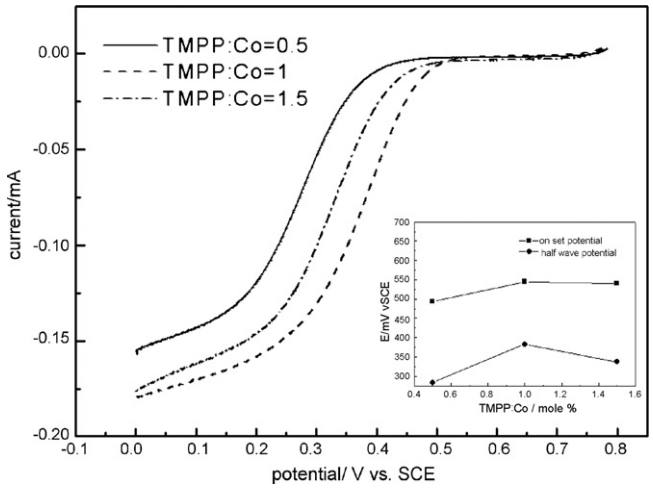

Fig. 6. Potentiodynamic curves for ORR on catalysts with different contents of TMPP. Inset shows change of onset potential and half-wave potential vs. content of TMPP.

although acidic media is used in this work. Thus, the evolution of catalytic activity does not follow the increasing TMPP:Co mole ratio as expected. The explanation for this result is that N contents beyond saturation are catalytically inactive after all the utilizable metal is coordinated with N. These excess amounts of TMPP may modify the microstructure of the carbon during high-temperature pyrolysis by blocking the active sites and there by result in the decrease of catalytic activity.

From the above experiments on the catalysts with different metal and nitrogen contents, it is known that a higher content of precursors does not necessarily yield higher activity. It depends on the utilizable amount in the active sites. Further addition of these precursors during catalyst synthesis either has no effect or has an adverse effect on the activity.

4. Conclusions

The origin of the ORR activity of the macrocycle composite catalyst comes from the simultaneous presence of a metal precursor, active carbon and a nitrogen source in the micropores. This work has investigated the effects of various parameters during the synthesis of the composite catalyst. The activity of catalysts is related to the mechanically mixing methods, the solvent used, the pyrolysis temperature, the metal content, and the nitrogen content. A pyrolyzed mixture synthesized by ultrasonication displays better activity for ORR than that achieved by ball milling. It is not critical to the formation of active catalytic sites whether macrocycles are soluble in the solvents or not. Instead, catalyst synthesized with different solvents show different surface area of micropores, the change of which correlates well with the activity. Heat treatment is a key step to the formation of active catalytic sites and the optimum pyrolysis temperature is 600 °C. Maximum activity is found at a 1:1 TMPP:Co mole ratio and a 5 wt.% Co/carbon weight ratio.

Acknowledgements

This work is supported by the Startup-grant of Nanyang Technological University, Academic research fund AcRF tier 1(RG40/05) and AcRF tier 2 (ARC11/06), Ministry of Education, Singapore. The authors are also grateful for financial support of this work from the National Science Foundation of China (20776085, 20060248064), the Science & Technology Commission of Shanghai Municipality (06SN07115, 065211020) and the 863 Project of China (2007AA05Z145).

References

[1] L. Zhang, J. Zhang, D.P. Wilkison, H. Wang, J. Power Sources 156 (2006) 1712.
[2] F. Jaouen, J.-P. Dodelet, Electrochim. Acta 52 (2007) 5975.
[3] S. Gottesfeld, T.A. Zawodzinski, Adv. Eletrochem. Sci. Eng. 5 (1997) 195.
[4] Wolf Vielstich, Arnold Lamm, Hubert Gasteiger, Handbook of Fuel Cells-Fundamentals Technology and Applications, Wiley, vol. 3, 2003 (Chapters 37–41).
[5] J. Roser, G. Zettisch, J. Scholta, L. Jorissen, J. Garche, International Conference with Exhibition, Fuel Cell 2000 Proceedings, 2000, pp. 75–83.
[6] O. Solorza-Feria, K. Ellmer, M. Giersig, N. Alonso-Vante, Eletrochim. Acta 39 (1994) 1647.
[7] R.W. Reeve, P.A. Christensen, A. Hamnett, S.A. Haydock, S.C. Roy, J. Electrochem. Soc. 145 (1998) 3463.
[8] J.M. Zen, C.B. Wang, J. Eletrochem. Soc. 141 (1994) L51.
[9] M.C. Martins Alves, J.P. Melet, D. Guay, M. Ladouceur, G. Tourillon, J. Phys. Chem. 96 (1992) 10898.
[10] L.T. Weng, P. Bertrand, G. Lalande, D. Guay, J.P. Domelet, Appl. Surf. Sci. 84 (1995) 9.
[11] H.X. Zhong, H.M. Zhang, G. Liu, Y.M. Liang, J.W. Hu, B.L. Yi, Eletrochem. Commun. 8 (2006) 707.
[12] A.L. Bouwkamp-Wijnoltz, W. Visscher, J.A.R. van Veen, Electrochim. Acta 43 (1998) 3141.
[13] P. Gouérec, M. Savy, J. Riga, Electrochim. Acta 44 (1998) 743.
[14] O. Contamin, C. Debiemme-Chouvy, M. Savy, G. Scarbeck, J. New Mater. Electrochem. Syst. 3 (2000) 67.

[15] F. Jaouen, S. Marcotte, J.-P. Dodelet, G. Lindbergh, J. Phys. Chem. B 107 (2003) 1376.
[16] G. Faubert, G. Lalande, R. Cote, D. Guay, J.-P. Dodelet, L.T. Weng, P. Bertrand, G. Denes, Electrochim. Acta 41 (1996) 1689.
[17] G. Lalande, R. Cote, G. Tamizhamni, D. Guay, J.-P. Dodelet, L. Dignard-Bailey, L.T. Weng, P. Bertrand, Electrochim. Acta 40 (1995) 2635.
[18] M. Bron, S. Fiechter, M. Hilgendorff, P. Bogdanoff, J. Appl. Electrochem. 32 (2002) 211.
[19] M. Lefevre, J.-P. Dodelet, P. Bertrand, J. Phys. Chem. 104 (2000) 1123.
[20] A.L. Bouwkamp-Wijnoltz, W. Visscher, J.A.P. van Veen, S.C. Tang, Electrochim. Acta 45 (1999) 379.
[21] C. Mocchi, S. Trasatti, J. Mol. Catal. A: Chem. 204–205 (2003) 713.
[22] Z. Ma, X. Xie, X. Ma, D. Zhang, Q. Ren, N. Heß-Mohr, V.M. Schmidt, Electrochem. Commun. 8 (2006) 389.
[23] G. Faubert, S. Gupta, R.F. Savinell, J. Electroanal. Chem. 462 (1999) 63.
[24] F. Jaouen, M. Lefevre, J.-P. Dodelet, M. Cai, J. Phys. Chem. B 110 (2006) 5553.
[25] F. Jaouen, J.-P. Dodelet, J. Phys. Chem. 111 (2007) 5963.
[26] J.-P. Dodelet, Oxygen reduction in PEM fuel cell conditions: heat-treated non-precious metal-N4 macrocycles and beyond, in: N4-Macrocyclis Metal Complexes: Electrocatalysis, Electrophotochemistry, and Biomimetic Electroanalysis, Springer Science and Business Media Inc., New York, 2006 (Chapter 3).